11

Comparison of Numerical Simulations and Ultrasonography Measurements of the Blood Flow through Vertebral Arteries

Damian Obidowski and Krzysztof Jozwik
Technical University of Lodz,
Institute of Turbomachinery, Medical Apparatus Division
Poland

1. Introduction

Vertebral arteries are a system of two blood vessels through which blood is carried to the rear region of the brain. This region of the human body has to be very well supplied with blood. Blood is delivered to the brain through carotid arteries as well. Due to their position and shape, vertebral arteries are a special kind of blood vessels. They have their origin at a various distance from the aortic ostium, can branch off at different angles, and have various lengths, inner diameters and spatial shapes. The above-mentioned variations are connected with inter-patient differences in the human anatomy. In the upper part of vertebral arteries, there is a marked arch curvature, owing to which turning the head is not followed by obliteration of these vessels. Contrary to other arteries, vertebral arteries join at their ends to form one vessel, a comparatively large basilar artery. This junction can be characterized by a varied geometry as well. For individual geometrical configurations of the vertebral artery system, there are also differences in the diameter of the left and right artery. All the above-mentioned differences result from a unique individual anatomical structure and do not follow from any pathology (Daseler & Anson 1959; Jozwik & Obidowski 2008; Jozwik & Obidowski 2010).

Some symptoms occurring in patients may suggest that the cause of an ailment lies in an incorrect blood supply to the rear region of the brain, and thus in an incorrect blood flow through vertebral arteries. The direct cause of such a phenomenon can result from arterial occlusion. The ultrasonography is employed to check the flow correctness. It is rather difficult to conduct this imaging procedure, but if it is performed by an experienced specialist, then the results obtained can be considered reliable. It happens, however, that the measured values of the maximum and minimum velocity in the left and right artery, which characterize the blood flow, differ significantly. Hence, the diagnosis of arteriosclerosis in these vessels is well based. It can be an indication for a surgical procedure (Mysior 2006). A significantly large percentage of cases diagnosed in such a way are not related to changes in the artery structure, and thus surgery would be irrelevant. If a structure and a shape of vertebral arteries, their individual variations are considered, then differences in the blood flow and a lack of relation between these differences and artery diameters can result from flow phenomena only.

The aim of the present study is to investigate the hydrodynamics of the blood flow through three different kinds of artery geometries to have a better insight into the phenomena occurring in the human body and to compare these simulation results with results of ultrasonography measurements (Jozwik & Obidowski 2008, Jozwik & Obidowski 2010).

2. Structure of vertebral arteries

In the human anatomical structure, several basic types of the spatial geometry in vertebral arteries can be differentiated. A frequency of their occurrence varies and one can say that three or four of them at most refer to the majority of cases met. Figure 1 presents types of the geometrical structure of vertebral arteries and a percentage of their occurrence in population.

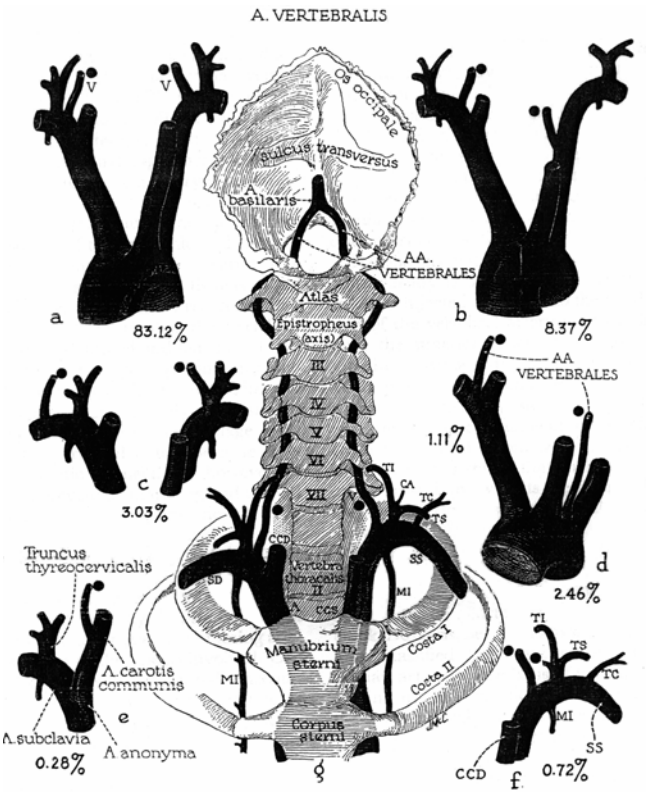

Fig. 1. Types of the vertebral artery structure and a percentage of their occurrence in population: a) the most frequently appearing case, b) the left artery starting significantly below, c) the right artery starting from the point far from the origin of carotid arteries, d) the left artery starting from the aortic arch, e, f, g) other structures resulting in less than 1% cases (Daseler & Anson 1959)

An essential aspect of the structure of vertebral arteries is their 3D characteristic curve. For a given type of the vertebral artery structure, there occur differences, often significant, in

inner diameters (left to right and patient to patient), and thus in flow fields. Such variations in inner diameters do not exceed the range of 2 – 6 mm. However, for a particular patient anatomy, the inner diameter, except for stenosis occurring in arteries, of an individual vertebral artery can be treated as constant along the artery. Nevertheless, it is impossible to formulate explicit relations describing the dependence between the left and right artery inner diameter. Each configuration of diameters (whose values fall within the range mentioned) is possible (Daseler & Anson 1959; Sokołowska 1988).

3. Model of the selected structure geometry

For the system of the vertebral artery structure occurring most frequently in the human anatomical structure, three models of its geometry have been developed (see Fig. 2). Each model has one inlet (aortic ostium) and six outlets (cross-sections of main arteries in the considered region). Owing to a significant differentiation in individual human anatomy (Daseler and Anson 1959; Ravensbergen et al.1974), which consists in a varied arrangement, length, kind of junctions, inner diameters and other geometrical parameters of the blood vessels under consideration, averaged data included in anatomical atlases, scientific publications, results of tomographic, magnetic resonance and ultrasonography imaging (Daseler and Anson 1959; Bochenek and Reicher 1974; Daniel 1988; Michajlik and Ramotowski 1996; Sinelnikov 1989; Vajda 1989) have been employed in the models developed. The models of vertebral arteries do not account for a part of secondary vessels branching off from the arteries under analysis before they join to form the basilar artery. Diameters of these vessels are relatively very small and their effect on the flow is insignificant.

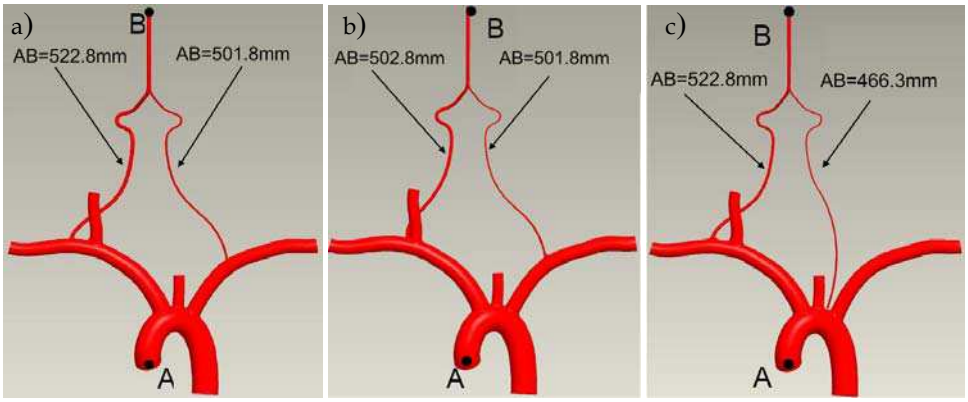

Fig. 2. Developed models of the selected geometry of the vertebral artery region of the circulatory system (Obidowski 2007)

The 3D shape of arteries has been taken into account in the three models prepared. These models differ as far as the place the left and right artery starts, the spatial shape and the length of individual arteries are concerned. For each model further on referred to as model 1, 2 and 3, differences in the total length of the left and right artery occur that are equal to, respectively: for model 1 – left artery – 501.8 mm, right artery – 522.8 mm, for model 2 – left artery – 501.8 mm, right artery – 502.8 mm, for model 3 – left artery – 466.3 mm, right artery

– 522.8 mm. These differences result from various places the left or right vertebral artery originates. Model 3, in which the left artery starts directly on the aortic arch, differs mostly. Moreover, it has been assumed that artery diameters can vary within the range of the values quoted above, but they are constant along their length. Taking into consideration changes in the inner diameter with a step equal to 1 mm and the fact that an arbitrary combination of the left and right artery diameter can occur, 25 cases of geometry for each model system and three different system geometries have been obtained, giving altogether 75 cases to be analysed. To simulate the flow, walls of all vessels considered have been assumed rigid and not subject to deformations with changes in the blood pressure. The diameters of the remaining artery vessels in the segments under consideration are listed in Table 1.

Artery	Diameter [mm]
Aorta	28.5
Brachiocephalic trunk artery	20 at bifurcation ÷ 14 at the outlet cross-section
Right carotid artery	14 at bifurcation ÷ 12 at the outlet cross-section
Left carotid artery	12 at bifurcation ÷ 11.5 at the outlet cross-section
Left subclavian artery	16 at bifurcation ÷ 15.5 at the outlet cross-section
Basilar artery	3 ÷ 8.5 depending on the vertebral artery diameter
Vertebral arteries	2 ÷ 6 depending on the case studied

Table 1. Values of diameters used to model the geometry (Bochenek 1974; Daniel 1988; Mysior 2006; Vajda 1989 et al.)

For each case of the system geometry, a computational mesh built of tetrahedral elements, condensed in the region of vertebral arteries, has been generated. Additionally, prism elements have been introduced in the vicinity of walls to define flow parameters at vessel walls more precisely. A sample mesh can be found in (Obidowski 2007, Jozwik and Obidowski 2010). The mesh independence tests have not yielded any significant differences that could affect the results of the computations conducted. Thus, due to time-consuming transient simulations, a middle-size density has been employed. The average size of the mesh used is approx. 1 million elements.

4. Blood flow parameters and boundary conditions

Blood is the medium owing to which each place in our organism is supplied with products indispensable for life and simultaneously purified from waste or toxic substances. From the viewpoint of flow, blood parameters are very difficult to describe. Even for a particular individual, values of the parameters alter, and these alterations depend on numerous factors connected with sex, age, diet and physical conditions, etc. Moreover, variations in values of blood flow parameters occur both slowly (e.g., along with the patient's ageing), as well as very fast (e.g., as an effect of irritation). The blood flow in human body is a cyclic flow with a strong asymmetry of changes within one cycle. In addition, owing to damping properties of blood vessel walls, amplitude and pressure variations versus time undergo changes depending on a position and a distance of the point under consideration from the heart. A proper model of blood, as well as properly imposed boundary conditions exert a direct

influence on the quality and accuracy of computations (Ballyk et al. 1994; Chen & Lu 2006; Gijsen et al. 1999; Johnston et al. 2004; Obidowski 2007, Walburn & Schneck 1976). On the other hand, taking into account a relatively wide range of alternations in values of these parameters, the blood model should reflect its behaviour in the flow and not necessarily render exactly the values of individual quantities that describe blood flow characteristics.

4.1 Model of blood

From the viewpoint of flow, the fundamental blood parameters are as follows:

- density,
- viscosity,
- heat conductivity.

For the phenomena and the region under consideration, the last parameter can be neglected. Changes in blood density depend on age and sex of the person first of all and their values fall within the range of 1030 – 1070 kg/m^3 (Bochenek et al. 1974, Michajlik et al. 1996). For the needs of this simulation, the constant density of blood equal to 1055 kg/m^3 has been assumed.

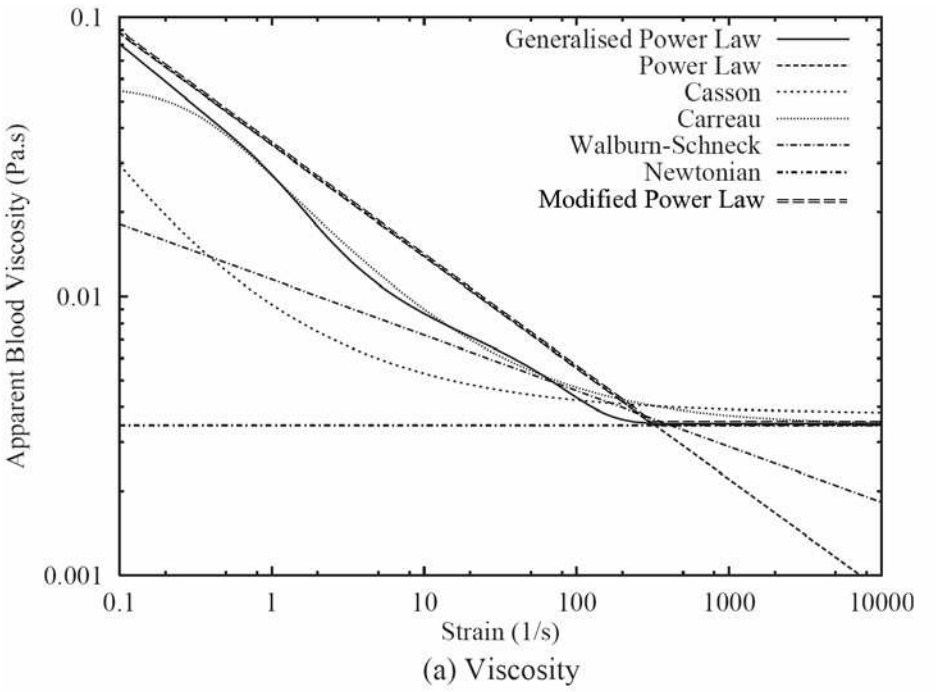

Fig. 3. Apparent blood viscosity as a function of strain for different blood models (Johnston et al. 2004)

Blood is a non-Newtonian fluid with a state memory. It means that the dynamic viscosity coefficient does not depend on the kind of liquid only, but also on flow parameters and a tendency in their variations. In the literature, numerous models describing a relation between the blood viscosity coefficient and blood flow parameters can be found. To describe

the flow occurring in vicinity of the aortic ostium, the Newton's model is appropriate. On the other hand, the blood flow in small vessels needs a more complex blood model (Ballyk et al. 1994; Chen and Lu 2006; Gijsen et al. 1999; Johnston et al. 2004; Obidowski 2007, Walburn and Schneck 1976). For the purpose of this study, a modified Power Law model has been employed. This model reflects the behaviour of the Newtonian fluid for large Reynolds numbers and simultaneously renders the flow nature at the viscosity of blood vessels of low diameters and low velocities. The model is expressed by the following system of equations:

$$\begin{cases} \mu = 0.554712 \text{ for } \left(2\dfrac{\partial U_i}{\partial x_j}S_{ij}\right)^{\frac{1}{2}} < 1e^{-9} \\ \mu = \mu_0\left(\left(2\dfrac{\partial U_i}{\partial x_j}S_{ij}\right)^{\frac{1}{2}}\right)^{n-1} \text{ for } 1e^{-9} \le \left(2\dfrac{\partial U_i}{\partial x_j}S_{ij}\right)^{\frac{1}{2}} < 327 \\ \mu = 0.00345 \text{ for } \left(2\dfrac{\partial U_i}{\partial x_j}S_{ij}\right)^{\frac{1}{2}} \ge 327 \end{cases} \quad (1)$$

where: = 0.0035 Pa s, n = 0.6 and $\left(2\dfrac{\partial U_i}{\partial x_j}S_{ij}\right)^{\frac{1}{2}}$ - shear strain rate.

Characteristic curves as a function of strain are presented in Fig. 3. The same curves show variations in other blood models known from the literature (Johnston et al. 2004; Gijsen et al. 1999; Walburn & Schneck 1976).

4.2 Boundary conditions

For the system under consideration, boundary conditions referring to time-variable parameters at the inlet and in six outlet cross-sections (see Fig. 4) should be assumed. Velocity variations versus time, as well as pressure variations can be approximated with a Fourier series. The Fourier series employed to determine the velocity and pressure waves takes the following form:

$$F(t) = \frac{1}{2}a_0 + \sum_{n=1}^{3}\left(a_n\cos(n\omega t + t_0) + b_n\sin(n\omega t + t_0)\right) \quad (2)$$

where a_0, a_n and b_n are experimentally determined Fourier coefficients and t_0 is a phase displacement. Thus, at the inlet, that is to say, at the aortic ostium, a uniform velocity distribution for the whole cross-section has been adopted. Six harmonics of the Fourier series allow one to generate a velocity profile used in the presented experiment as shown in Fig. 5, which is an approximation of experimental curves found in the literature (Traczyk 1980, Viedma 1997).

The time-variable static pressure has been taken as the parameter determining boundary conditions at outlets. The static pressure also changes periodically and a time displacement of these changes following from various paths of the pulse wave measured from the aortic

ostium should be taken into account for the assumed outlet cross-sections. The values of phase displacements for individual outlet cross-sections have been calculated on the basis of the length of centre lines and pulse wave propagation velocities in arteries. Wang has determined pulse wave propagation velocities in individual human arteries (Wang 2004). For the outlet cross-section of the basilar artery, the pressure has been determined on the basis of the averaged path along the left and right vertebral artery. The static pressure variations for individual outlets are shown in Fig. 6 (Jozwik & Obidowski 2009).

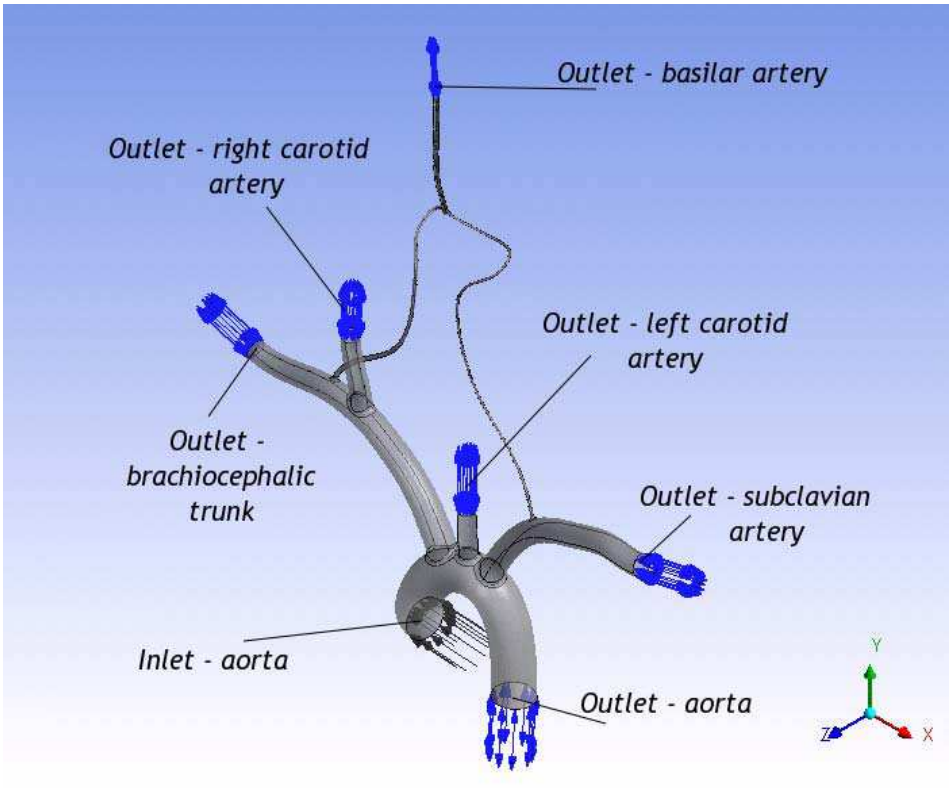

Fig. 4. Boundary conditions at the inlet and outlets of the modelled geometry of the vertebral arteries under investigation (Obidowski 2007)

The walls of vessels in which blood flows are supposed to be nondeformable. Owing to the flow nonstationarity that follows both from considerable values of velocity at the aortic ostium, numerous branches and narrowings, as well as from a pulsating nature of the flow, the flow is expected to be turbulent in many places of the system being modelled. A Shear Stress Transport (SST) model, belonging to the k-ω model family, has been adopted as the turbulence model in the investigations.
This model renders correctly the character of the boundary flow for the flows characterized by low Reynolds numbers. Initially, the calculations were conducted for the flow under steady conditions.

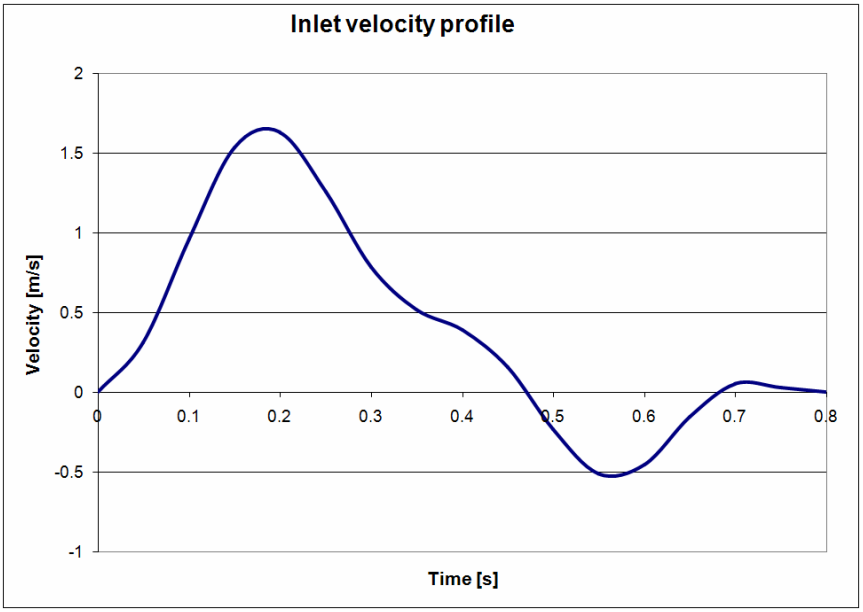

Fig. 5. Changes in velocity as a function of time for the inlet cross-section during one cycle of heart operation (Obidowski 2007)

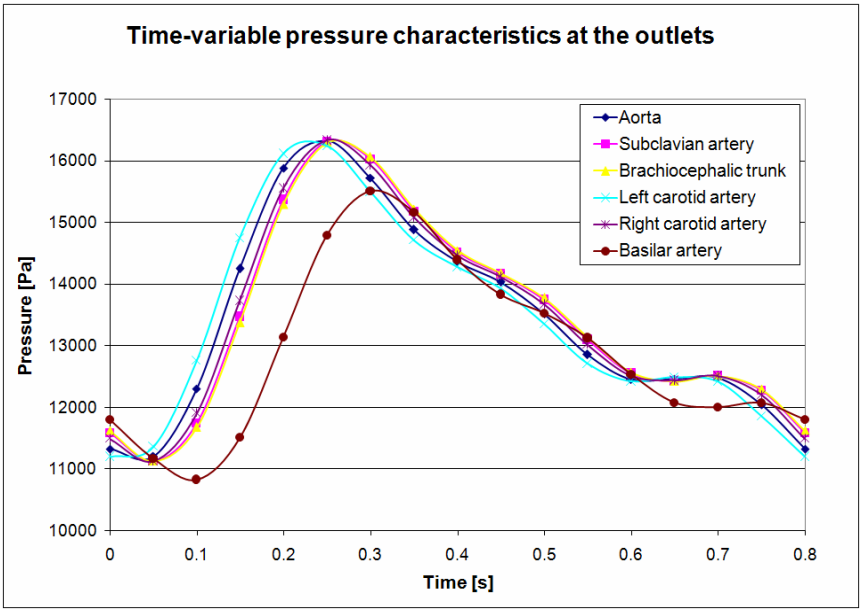

Fig. 6. Changes in pressure as a function of time for outlet cross-sections during one cycle of heart operation (Jozwik & Obidowski 2009)

The following values of parameters at the inlet and the outlet were taken, namely:
- velocity in the aortic ostium, v_{as} = 1.44 m/s,
- all static pressures in all outlet cross-sections were assigned to averaged static pressures and were equal to 13 kPa.

The results obtained for steady flow calculations were taken as the initial ones for the unsteady flow, for which the calculations of five cycles of variations in parameters were conducted. Owing to this, the obtained results are independent of the assumed initial values from the steady flow conditions.

4.3 Governing equations

The ANSYS CFX v. 10.0 solver was used to obtain a solution to the described problem. The unsteady Navier-Stokes equations in their conservation form are a set of equations solved by ANSYS CFX (ANSYS CFX-Solver Theory Guide).
The continuity equation is expressed as:

$$\frac{\partial \rho}{\partial t} + \nabla \cdot (\rho U) = 0 \tag{3}$$

Thus, the momentum equation takes the following form:

$$\frac{\partial (\rho U)}{\partial t} + \nabla \cdot (\rho U * U) = -\nabla p + \nabla \cdot \tau + S_M \tag{4}$$

where the stress tensor, τ, is related to the strain rate by the following relation:

$$\tau = \mu \left(\nabla U + (\nabla U)^T - \frac{2}{3} \delta \nabla \cdot U \right) \tag{5}$$

The total energy equation is represented by:

$$\frac{\partial (\rho h_{tot})}{\partial t} - \frac{\partial p}{\partial t} + \nabla \cdot (\rho U h_{tot}) = \nabla \cdot (\lambda \nabla T) + \nabla \cdot (U \cdot \tau) + U \cdot S_M + S_E \tag{6}$$

where h_{tot} is the total enthalpy, related to the static enthalpy h(T, p) by:

$$h_{tot} = h + \frac{1}{2} U^2 \tag{7}$$

The term $\nabla \cdot (U \cdot \tau)$ represents the work due to viscous stresses and is called the viscous work term. The term $U \cdot S_M$ refers to the work due to external momentum sources and is currently neglected.
An alternative form of the energy equation, which is suitable for low-velocity flows, is also available. To derive it, an equation for the mechanical energy K is required. This equation has the form:

$$K = \frac{1}{2} U^2 \tag{8}$$

The mechanical energy equation is derived by taking the dot product of U with the momentum equation:

$$\frac{\partial(\rho K)}{\partial t} + \nabla \cdot (\rho U K) = -U \cdot \nabla p + U \cdot (\nabla \cdot \tau) + U \cdot S_M \tag{9}$$

In the present paper, the thermal energy equation is not taken into consideration as the blood flow in the short time is isothermal, thus energy dissipation and heat conductivity is neglected.

5. Results

For the 75 model geometrical cases investigated that cover changes in inner diameters of vertebral arteries of the three selected types of their spatial geometry, the results that allow for an analysis of velocity distributions during the whole cycle of heart operation in an arbitrary point of the modelled system have been obtained. The distance of the origin of vertebral arteries from the aortic ostium enables one to determine proper velocity profiles at the points crucial from the viewpoint of the investigations conducted. As an example, velocity profiles determined in the left and right vertebral artery during the first phase of the simulated cycle of heart operation (range of 0.15 – 0.30 s) are depicted in Fig. 7. One can see the velocity profile that suggests a laminar flow for small diameters, whereas for large diameters of blood vessels, the obtained profiles are deformed by unsteadiness of the phenomena and an effect of the duct curvature can be observed.

Determination of the flow structure versus time at the point where vertebral arteries join to form the basilar artery is more important for the investigation. Figures 8 and 9 show various velocity profiles in this point for five time instants of the heart operation cycle for the selected geometrical variants of three modelled structures and two different diameters of left and right arteries (Fig. 8 shows distributions for the diameter of the left artery equal to 3 mm and the right one – 5 mm and Fig. 9 presents the different situation – the diameter of the left artery equals 4 mm and of the right one – 2 mm). A very strong disproportion of the velocity of blood flowing into the basilar artery from the left and right artery and between the same arteries in different models can be observed. Of course, the result obtained refers to the selected geometry and is not characteristic of all cases under consideration. A possibility to compare changes in velocity of the left and right artery during one cycle of heart operation for the three selected geometries and three modelled structures of vertebral arteries is provided by the distributions shown in Fig. 10.

An effect of the velocity increase cannot be observed in the artery with an increasing diameter. Even for the identical diameter of both arteries, the velocity profile differs significantly. For the constant diameter of the arteries, both the left and the right one (see Fig. 10 b and c), a change in the diameter of the second artery affects differently a change in the velocity in the artery under consideration. In the left vertebral artery, the maximum velocity is attained for the same diameter of both the arteries (4 mm), whereas for the right artery, such behaviour was observed for the largest diameter of the left artery (6 mm). In this case, differences between the velocities occurring for individual diameters of the left artery under analysis are considerably lower. For the given low, constant diameter of the left artery equal to 2 mm (see Fig. 10 a), the maximum velocity occurs for two values of the right artery diameter (4 and 6 mm). Here, for the diameter of the right artery equal to 5 mm, a sharp decrease in the maximum velocity value in the left artery occurs. An effect of wave phenomena on the flow in arteries can be clearly seen.

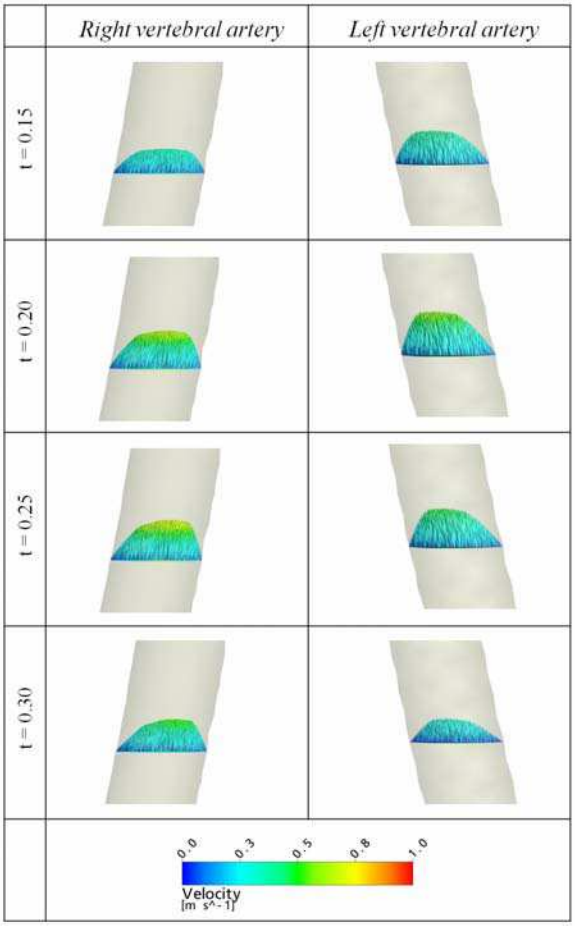

Fig. 7. Velocity distribution along the diameter of the left and right vertebral artery for one geometrical configuration at different instants of the heart operation cycle (t = 0.15 s, t = 0.2 s, t = 0.25 s, t = 0.3 s) (Obidowski 2007)

Some possibilities to compare the effect of diameters of the left and right vertebral artery on the values of velocity, which were obtained in these blood vessels during the simulations, are provided by a comparison of maximum velocities within the single heart cycle, measured in the centre part of the left and right artery for all the diameter configurations and for three modelled structures of these vessels analysed. This comparison is presented in Fig. 11 but only for the changes in the diameter from 2 to 5 mm as data from ultrasonography measurements were available only for this range. Moreover, the values of the maximum velocity for the defined diameters corresponding to the vessel diameters, calculated on the basis of the Hagen-Poiseuille equation, are shown. The equation is frequently used in medicine to compare the velocities in both the arteries (left and right) on the basis of the resistance assumed in vessels being a function of their diameters and a pressure drop in vertebral arteries.

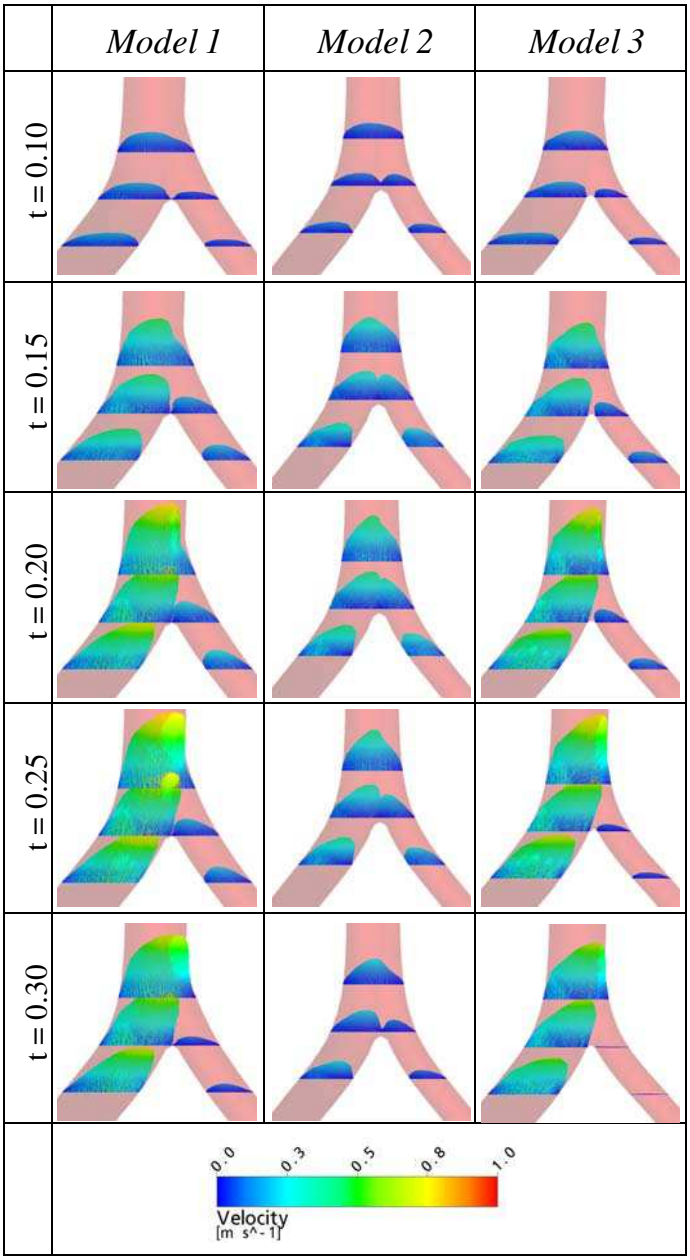

Fig. 8. Comparison of velocity profiles at the point vertebral arteries join to form the basilar artery for three spatial geometrical variants of the same diameter variant (left3right5) and for five time instants of the heart operation cycle (t = 0.1 s, t = 0.15 s, t = 0.2 s, t = 0.25 s, t = 0.3 s)

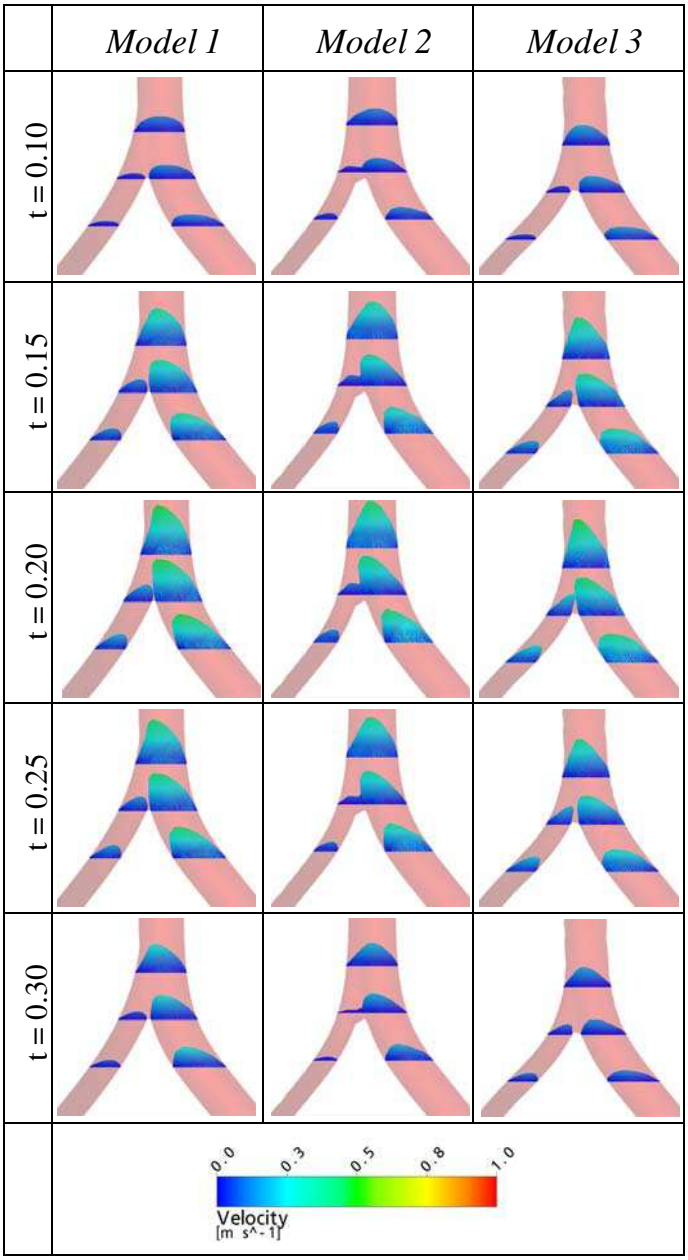

Fig. 9. Comparison of velocity profiles at the point vertebral arteries join to form the basilar artery for three spatial geometrical variants of the same diameter variant (left4right2) and for five time instants of the heart operation cycle (t = 0.1 s, t = 0.15 s, t = 0.2 s, t = 0.25 s, t = 0.3 s)

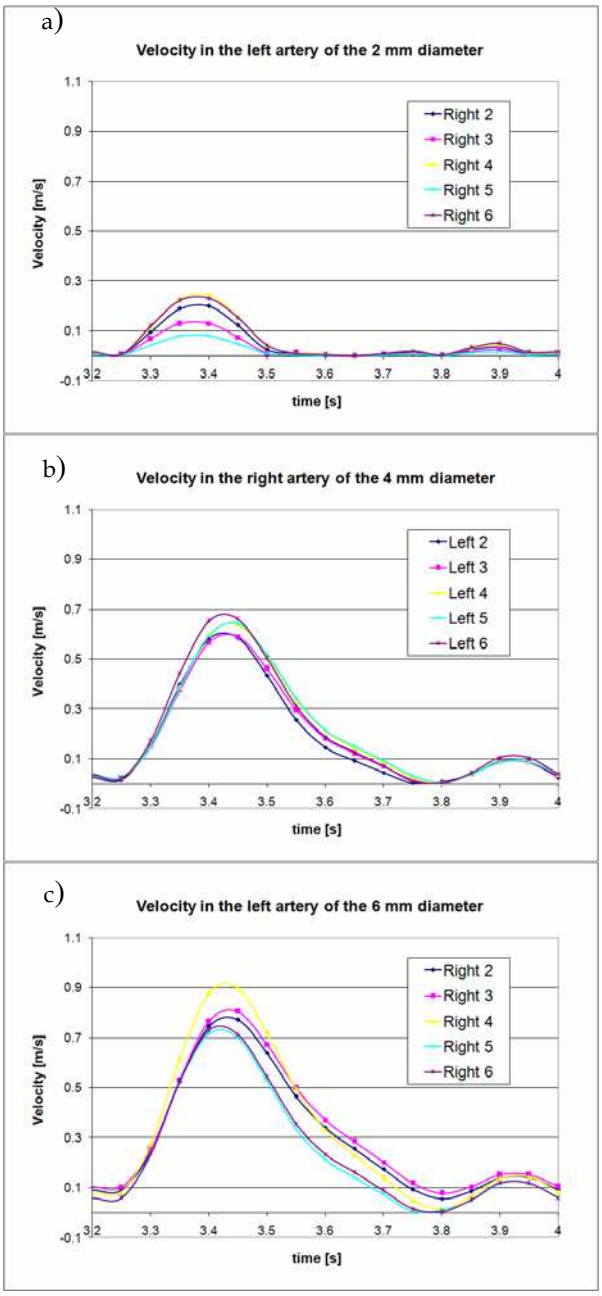

Fig. 10. Velocity distributions vs. time for one heart operation cycle in the left and right vertebral artery for three geometrical variants of blood vessels (left 2 mm, right 4 mm, left 6 mm) (Obidowski 2007)

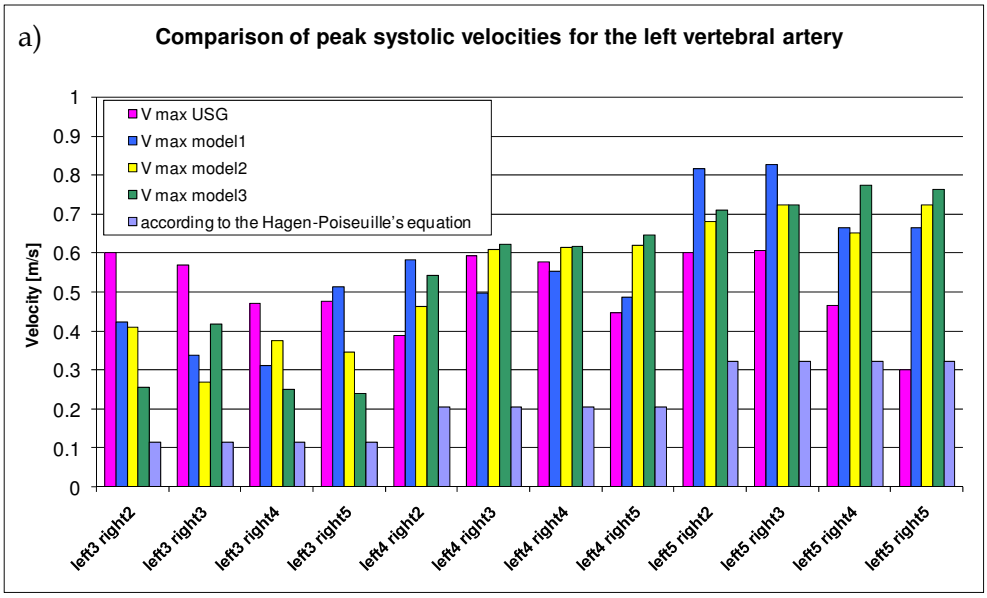

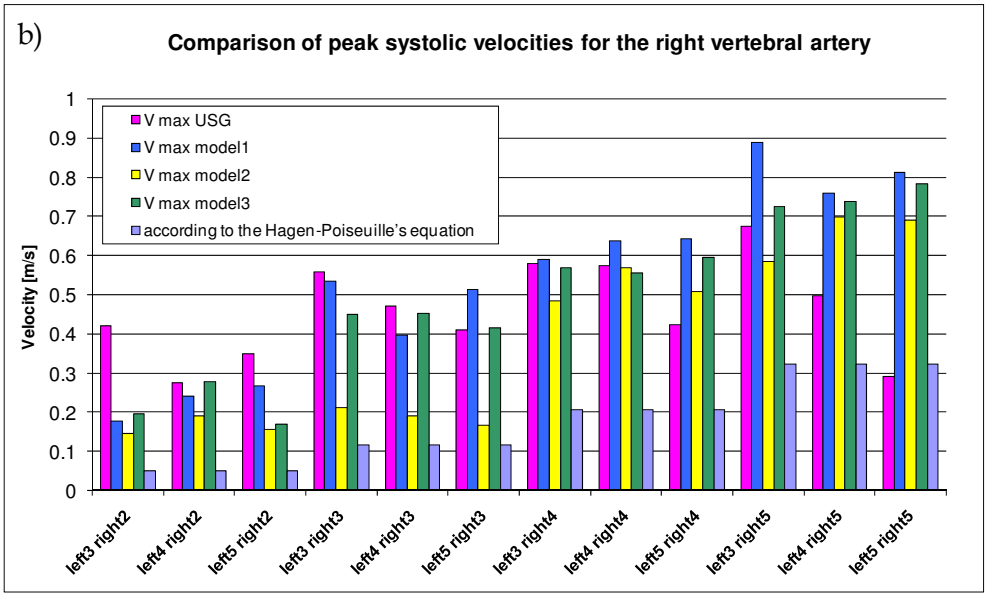

Fig. 11. Comparison of the maximum value of velocities obtained for the left and right vertebral artery for all investigated geometrical configurations of the system, ultrasonography measurements and calculated on the basis of the Hagen-Poiseuille equation (Obidowski 2007)

The same plot shows the maximum velocity values obtained from ultrasonography measurements in 520 people. The results have been averaged for all patients who had individual values of diameters of vertebral arteries, but without distinguishing the type of the spatial structure of arteries (Mysior 2006).
A good conformity between the results obtained from simulations and measurements (without distinguishing the type of geometry of arteries) occurs in the central region, which means a lack of conformity at the smallest diameters and for the two largest diameters. In case of large vertebral artery diameters, the results of measurements agree with those obtained on the basis of the Hagen-Poiseuille equation. For large diameters, an undisturbed laminar flow occurs, and thus the above-mentioned equation, which refers basically to such flows, yields correct results. A difference in the simulation results can follow from the fact that artery wall deformations have not been considered. It also refers to the case of the variant with the smallest diameters where the simulation results do not agree with the measurements. The vessel wall material is not subject to the Hook's law, and the relationship between the deformation and the pressure inside the vessel (or, strictly speaking, a difference in pressure between its inside and outside) is strongly nonlinear and dependent on the individual human anatomical structure. Thus, modelling the deformations in vertebral artery walls as a function of the flowing blood is extremely difficult if not impossible at all.

6. Discussion

The conducted numerical investigations confirm a possibility of modelling the geometry of the system of vertebral arteries together with vessels in their vicinity and of obtaining results that enable an analysis of the effect of an artery diameter on velocity distributions in vessels during the heart operation cycle for the selected, determined type of spatial geometry. The results obtained indicate explicitly that differences in the flow and instantaneous velocity values in vertebral arteries and in the point they join to form the basilar artery may not result from pathological changes in the artery system, but can follow from physical phenomena that occur in arteries as a consequence of the pulsating character of flow and the unique geometry, which is related to the individual human anatomical structure.
The presented results refer to selected models of the vertebral artery structure and do not account for changes in the length of individual arteries. Taking into account such a possibility of changes within one model of the system (not only vessel diameters are variable, but their length as well), the determination of the cause of disproportions found in the flow in vertebral arteries is very difficult and complex.
The maximum velocity in one vertebral artery is affected by the flow in the other one (see Fig. 11), thus the flow in the basilar artery strongly depends on the diameters and lengths of both vertebral arteries.
The results of calculations according to the Hagen-Poiseuille equation, commonly used in medicine for determination of the relation between flows in vertebral arteries, do not allow one even to predict the behaviour of the flow. All properties of the flow in such arteries are against the assumptions of the flow described by the above-mentioned equation. It is clearly visible that the results obtained in the presented investigations differ significantly from those calculated according to the Hagen-Poiseuille equation (see Fig. 11).
While analysing the obtained results, one should remember about the fact that rigid walls of vessels have been assumed. This assumption affects directly the lack of energy accumulation

during the cardiac contraction phase and its recovery during the heart relaxation. Moreover, rigid vessels do not cause damping of the phenomena occurring during the flow in vertebral arteries. Taking into account deformability of vessel walls through an introduction of their rigidity, it will be possible to obtain a better approximation. An influence of flexible walls of arteries should be especially observed in the values of minimum velocities of blood and in obtaining reverse flows in vertebral arteries. An influence of the brain supply by carotid arteries should be taken into account, as only completeness of the system will allow one to consider a possibility of occurrence of wave phenomena. As a result, these phenomena can be proven to follow from the pulsating flow and the vessel geometry.
In order to evaluate the simulation results, a model of the actual system of vessels for the selected patient should be developed. Flows in vertebral arteries and blood systolic and diastolic pressure should be measured for the selected geometry and, on this basis, the boundary and initial conditions for the simulation should be defined. Only thus prepared models and data will enable a correlation of the results of calculations and measurements.

7. Notations

$\alpha, \beta, \beta^{'}, \sigma_k, \sigma_{\varpi}$, – constants,
k – turbulence kinetic energy,
ω - turbulence frequency,
μ - dynamic viscosity,
μ_t - turbulence viscosity,
U - velocity vector,
ρ - density,
v_t - eddy viscosity,
S - invariant measure of the strain rate,
P_t - turbulence production due to viscous and buoyancy forces.

8. References

Ballyk P.D., Steinman D.A. & Ethier C.R. (1994). Simulation of non-Newtonian blood flow in an end-to-end anastomosis, *J. Biorheology* Vol., No., 31, pp. 565–586.

Bochenek A. & Reicher M. (1974). *Human anatomy*, volume III, PZWL, ed. V, Warsaw, (in Polish).

Chen J. & Lu X.Y., (2006). Numerical investigation of the non-Newtonian pulsatile blood flow in a bifurcation model with a non-planar branch, *J. Biomechanics*, Vol., No., 39, pp. 818 – 832.

Daniel B., (1988). *Atlas of human radiological anatomy*, PZWL, Warsaw, (in Polish).

Daseler E. H. & Anson B. J., (1959). Surgical anatomy of the subclavian artery and its branches, *Surgery, Gynecology & Obstetrics*, pp. 149-174.

Gijsen, F.J.H., van de Vosse, F.N. & Janssen, J.D. (1999). The Influence of the Non-Newtonian Properties of Blood on the Flow in Large Arteries: Steady Flow in a Carotid Bifurcation Model, *J. Biomechanics* Vol., No., 32, pp. 601–608.

Gijsen, F. J. H., Allanic, E., van de Vosse, F. N., & Janssen, J. D., (1999). The Influence of the Non-Newtonian Properties of Blood on the Flow in Large Arteries: Unsteady Flow in a 90° Curved Tube, *J. Biomechanics*, Vol., No., 32, pp. 705–713.

Johnston B. M., Johnston P. R., Corney S. & Kilpatrick D. (2004). Non-Newtonian blood flow in human right coronary arteries: steady state simulations, *J. Biomechanics* Vol. No., 37, pp. 709-720.

Jozwik K. & Obidowski D., (2008). Geometrical models of vertebral arteries and numerical simulations of the blood flow through them, *Proceedings of BioMed2008, 3rd Frontiers in Biomedical Devices Conference & Exhibition*, pp. 5., BioMed2008-38048, ISBN 0-7918-3823-4, Irvine, California, USA, June 2008, ASME.

Jozwik K. & Obidowski D., (2009). Numerical simulations of the blood flow through vertebral arteries. *J. Biomechanics*, Vol., No., 43, pp. 177-185.

Michajlik A. & Ramotowski W. (1996). *Human anatomy and physiology,* PZWL, pp. 354-356 (in Polish).

Mysior M., (2006). *Doppler ultrasound criteria of physiological flow in asymmetrical vertebral arteries*, PhD Thesis, Polish Mother Memorial Research Institute, Lodz, 2006 (in Polish).

Obidowski D., (2007). *Blood flow simulation in human vertebral arteries,* PhD Thesis, Technical University of Lodz, Lodz, 2007 (in Polish).

Obidowski D., Mysior M., Jozwik K., (2008). Comparison of Ultrasonic Measurements and Numerical Simulation Results of the Flow through Vertebral Arteries, *Proceedings of 4th Conference of the International Federation for Medical and Biological Engineering*, pp. 23-27, Belgium, Antwerp, November 2008, IFMBE Vol. 22, pp. 286-292, Springer-Verlag Berlin, Heidelberg, 2009.

Ravensbergen J., Krijger J.K.B., Hillen B., Hoogstraten H.W. (1996). The Influence of the Angle of Confluence on the Flow in a Vertebro-Basilar Junction Model. *J. Biomechanics*, Vol., No., 29, pp. 281-299

Sinelnikov R.D., (1989). *Atlas of human anatomy*, Mir Publishers, Moscow.

Sokołowska J. - Pituchowa (eds.), (1988). *Human anatomy*, PZWL, Warsaw, (in Polish).

Traczyk W., Trzebski A., (1980). *Human physiology with elements of clinical physiology*, PZWL, Warsaw 1980 (in Polish).

Vajda J., (1989). *Atlas of human anatomy*, Akademia Kiodo, Budapest (in Polish).

Viedma A., Jimenez-Ortiz C. & Marco V., (1997). Extended Willis circle model to explain clinical observations in periorbital arterial flow. *J. Biomechanics*, Vol., No., 30, pp. 265-272.

Wang J.J. & Parker K.H. (2004). Wave propagation in a model of the arterial circulation. *J. Biomechanics*, Vol., No., 37, pp. 457-470.

Walburn, F.J. & Schneck, D.J. (1976). A constitutive equation for whole human blood. *Biorheology* Vol., No., 31, pp. 201-218.

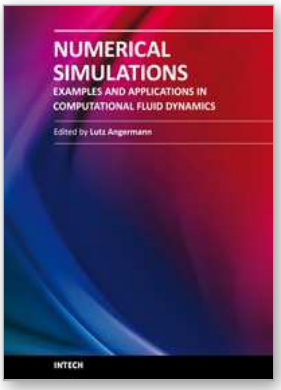

Numerical Simulations - Examples and Applications in Computational Fluid Dynamics

Edited by Prof. Lutz Angermann

ISBN 978-953-307-153-4
Hard cover, 440 pages
Publisher InTech
Published online 30, November, 2010
Published in print edition November, 2010

This book will interest researchers, scientists, engineers and graduate students in many disciplines, who make use of mathematical modeling and computer simulation. Although it represents only a small sample of the research activity on numerical simulations, the book will certainly serve as a valuable tool for researchers interested in getting involved in this multidisciplinary ï¬eld. It will be useful to encourage further experimental and theoretical researches in the above mentioned areas of numerical simulation.

How to reference

In order to correctly reference this scholarly work, feel free to copy and paste the following:

Damian Obidowski and Krzystof Jozwik (2010). Comparison of Numerical Simulations and Ultrasonography Measurements of the Blood Flow through Vertebral Arteries, Numerical Simulations - Examples and Applications in Computational Fluid Dynamics, Prof. Lutz Angermann (Ed.), ISBN: 978-953-307-153-4, InTech, Available from: http://www.intechopen.com/books/numerical-simulations-examples-and-applications-in-computational-fluid-dynamics/comparison-of-numerical-simulations-and-ultrasonography-measurements-of-the-blood-flow-through-verte

INTECH
open science | open minds

InTech Europe
University Campus STeP Ri
Slavka Krautzeka 83/A
51000 Rijeka, Croatia
Phone: +385 (51) 770 447
Fax: +385 (51) 686 166
www.intechopen.com

InTech China
Unit 405, Office Block, Hotel Equatorial Shanghai
No.65, Yan An Road (West), Shanghai, 200040, China
中国上海市延安西路65号上海国际贵都大饭店办公楼405单元
Phone: +86-21-62489820
Fax: +86-21-62489821